

Broadband optical amplification in silicate glass-ceramic containing β -Ga₂O₃:Ni²⁺ nanocrystals

ShiFeng Zhou^a, HuaFang Dong^b, GaoFeng Feng^a, BoTao Wu^c, HePing Zeng^b and JianRong Qiu^a

^aState Key Laboratory of Silicon Materials, Zhejiang University, Hangzhou 310027, China

^bKey laboratory of Optical and Magnetic Resonance Spectroscopy, and Department of Physics, East China Normal University, Zhongshan North Road 3663, Shanghai 200062, China

^cShanghai Institute of Optics and Fine Mechanics, Chinese Academy of Sciences, Shanghai 201800, China
qjr@zju.edu.cn

Abstract: We demonstrate broadband optical amplification at 1.3 μm in silicate glass-ceramics containing β -Ga₂O₃:Ni²⁺ nanocrystals with 980 nm excitation for the first time. The optical gain efficiency is calculated to be about 0.283 cm^{-1} when the excitation power is 1.12 W. The optical gain shows similar wavelength dependence to luminescence properties.

©2007 Optical Society of America

OCIS codes: (300.2140) Emission, (160.2750) Glass and other amorphous materials.

References and links

1. L. R. Pinckney and G. H. Beall, "Transition element-doped crystals in glass," Proc. SPIE **4452**, 93-99 (2001).
2. S. Kück, "Laser-related spectroscopy of ion-doped crystals for tunable solid-state lasers," Appl. Phys. B **72**, 515-562 (2001).
3. T. Suzuki, K. Horibuchi, and Y. Ohishi, "Structural and optical properties of ZnO-Al₂O₃-SiO₂ system glass-ceramic containing Ni²⁺-doped nanocrystals," J. Non-Crys. Solids **351**, 2304-2309 (2005).
4. T. Suzuki, G. S. Murugan, and Y. Ohishi, "Optical properties of transparent Li₂O-Ga₂O₃-SiO₂ glass-ceramics embedding Ni-doped nanocrystals," Appl. Phys. Lett. **86**, 131903 (2005).
5. Y. Wang and J. Ohwaki, "New transparent vitroceraamics codoped with Er³⁺ and Yb³⁺ for efficient frequency upconversion," Appl. Phys. Lett. **63**, 3268-3270 (1993).
6. S. F. Zhou *et al.*, J. Phys. Chem. C, accepted.
7. L. Galois and G. Calas, "Structural environment of nickel in silicate glass/melt systems: Part 1. Spectroscopic determination of coordination states," Geochim. Cosmochim. Acta **57**, 3613-3626 (1993).
8. N. Jiang *et al.*, submitted to Appl. Phys. Lett.
9. M. V. Iverson, J. C. Windscheif, and W. A. Sibley, "Optical parameters for the MgO:Ni²⁺ laser system," Appl. Phys. Lett. **36**, 183-184 (1980).
10. Y. Suzuki, W. A. Sibley, O. H. El Bayoumi, T. M. Roberts, and B. Bendow, "Optical properties of transition-metal ions in zirconium-based metal fluoride glasses and MgF₂ crystals," Phys. Rev. B **35**, 4472-4482 (1987).
11. C. Anino, J. Théry, and D. Vivien, "Cr⁴⁺ doped Li₂MgSiO₄, a new potential tunable laser material with room temperature fluorescence lifetime > 100 μs ," Proc. SPIE **3176**, 38-41 (1996).
12. H. Shigemura, M. Shojiya, R. Kanno, Y. Kawamoto, K. Kadono, and M. Takahashi, "Optical property and local environment of Ni²⁺ in fluoride glasses," J. Phys. Chem. B **102**, 1920-1925 (1998).
13. S. F. Zhou *et al.*, to be submitted
14. N. F. Mott and R. W. Gurney, *Electronic Processes in Ionic Crystals*; (Oxford, 1948).
15. M. Hughes, H. Rutt, D. Hewak, and R. J. Curry, "Spectroscopy of vanadium (III) doped gallium lanthanum sulphide chalcogenide glass," Appl. Phys. Lett. **90**, 031108 (2007).
16. B. N. Samson, L. R. Pinckney, J. Wang, G. H. Beall, and N. F. Borrelli, "Nickel-doped nanocrystalline glass-ceramic fiber," Opt. Lett. **27**, 1309-1311 (2002).
17. Y. Miyajima, T. Sugawa, and Y. Fukasaku, "38.2 dB amplification at 1.31 μm and possibility of 0.98 μm pumping in Pr³⁺-doped fluoride fibre," Electron. Lett. **27**, 1706-1707 (1991).
18. T. J. Whitley, "A review of recent system demonstrations incorporating 1.3 μm praseodymium-doped fluoride fiber amplifiers," J. Lightw. Technol. **13**, 744-760 (1995).

1. Introduction

The requirement to improve solid-state lasers, optoelectronic communication devices has renewed the interest in activator doped glass. Glass ceramic (GC) materials are one of the most important hybrid optical materials which can be produced by controlled nucleation and crystallization of glass. This class of nanocomposite materials can interestingly be used as hosts for activators because they can potentially combine the advantages of both glass (such as easy fabrication) and doped crystal (such as optical activity) [1].

Transition metals (TM) ions such as Ni^{2+} and Cr^{4+} are important activators since they show broadband luminescence in the near infrared region when incorporated into crystal matrices [2]. Unfortunately, TM ions only exhibit weak or even no luminescence in amorphous hosts, owing to the strong nonradiative relaxation. GC offers a potential solution to these problems. The design of novel matrix for TM ions is ultimately limited by two mechanisms. The first one is the necessity of certain crystal field environments, e.g. tetrahedral environment for Cr^{4+} and octahedral environment for Ni^{2+} [1, 3, 4]. The second one is nonradiative decay processes, which limit the quantum efficiency of TM ions in matrix. The requirement of certain crystal field environment indicates that the well studied transparent oxyfluoride GCs [5], which often provide 8-fold coordinated environment, are probably not suitable hosts for TM ions luminescence. To our knowledge, the GC matrixes for Cr^{4+} were mainly focused on forsterite, willemite and mixed orthosilicates and for Ni^{2+} was limited on spinel [1]. At present, the relative high luminescence quantum efficiency was reported for Ni^{2+} doped GC materials in Ref. [4]. Thus far, however, there are no reports about the realization of optical amplification in this class of hybrid optical materials. In this letter, we demonstrate an optical amplification at 1.3 μm in silicate GC containing $\beta\text{-Ga}_2\text{O}_3\text{:Ni}^{2+}$ nanocrystals.

2. Experimental

Ni^{2+} -doped silicate glass sample was prepared by the conventional melting-quenching technique. The glass composition was 66.5 SiO_2 -19.5 Ga_2O_3 -6.5 Al_2O_3 -7.5 Na_2O (mol%), doped with 0.15 mol% NiO. A mixture of SiO_2 (A.R.), Al_2O_3 (A.R.), Na_2CO_3 (A.R.), Ga_2O_3 (5N) and NiO (4N) was melted in a corundum crucible at 1680 °C for 2 h at ambient temperature. The glass samples were then obtained by rapidly quenching the melt to room temperature and annealing at 400 °C for 10 h. Characteristic temperatures were measured by differential thermal analysis (DTA) at a heating rate of 10 °C/min under N_2 atmosphere. The Ga_2O_3 nanocrystals were precipitated by heat treatment of the glass samples at 900 °C for 2 h. The sample was then cut and polished.

3. Results and discussion

From DTA measurement, glass transition temperature (T_g), first crystallization temperature (T_{c1}) due to the precipitation of $\beta\text{-Ga}_2\text{O}_3$ crystals, and second crystallization temperature (T_{c2}) corresponding to the crystallization of the glass matrix is 650 °C, 900 °C and 1150 °C, respectively. The XRD results show that the as-made glass is amorphous, while sharp diffraction peaks appear in the XRD pattern of the glass ceramic heat-treated at 900 °C for 2 h and all of them can be indexed by the diffraction peaks of monoclinic $\beta\text{-Ga}_2\text{O}_3$ structure. TEM results show that $\beta\text{-Ga}_2\text{O}_3$ particles have a relatively uniform diameter of about 50 nm. The detailed structural characterization of the glass ceramics can be found in Ref. [6].

Figure 1 shows the transmittance and absorption spectra of as-made glass and GC measured by a double-beam spectrophotometer (JASCO FP-6500). The transmittance of the GC is more than 90%. As shown in the inset of Fig. 1, the crystallization process has changed the absorption spectrum of glass. Just like other TM ions, Ni^{2+} is sensitive to crystal field because their valent electrons lack of shielding from surrounding crystal fields and the phenomenon is ascribed to the change of Ni-ion environment [4]. The absorption bands centered at 440, 880 and 1750 nm in the as-made glass can be ascribed to the trigonal bipyramid fivefold and tetrahedral fourfold Ni^{2+} ions in silicate glasses [7]. The broad

absorption bands at 1011 and 606 nm in GC can be attributed to transitions from ${}^3A_2(F)$ ground state to the ${}^3T_2(F)$ and ${}^3T_1(F)$ excited states of octahedral Ni^{2+} [4]. It is supposed that Ni^{2+} substituted Ga^{3+} since Ga atoms occupy both octahedral and tetrahedral sites in $\beta\text{-Ga}_2\text{O}_3$ [8]. Pumped by a common commercial semiconductor at 980 nm, GC shows intense broadband emission centered around at about 1200 nm. The fluorescent lifetime is more than 665 μs at room temperature. On contrast, the as-made glass shows no emission in the near-infrared wavelength region.

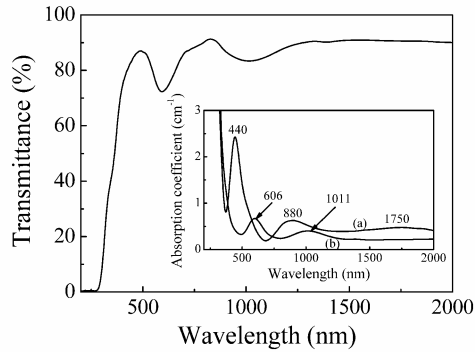


Fig. 1. Transmittance spectra of Ni-doped GC containing $\beta\text{-Ga}_2\text{O}_3$ nanocrystals. The inset shows the absorption spectra of Ni-doped (a) as-made glass and (b) GC. Sample thickness: 2 mm.

A configuration resembling a traditional two-wave mixing geometry was chosen in gain measurements (shown in the Fig. 2). The thickness of sample for gain measurement was 4 mm. A tunable laser diode (New Focus Inc. 6324, 0.3 nm width) was used as seed source, in which the tunable region is from 1272 to 1348 nm. The seed beam was chopped at 200 Hz by a chopper (Stanford Research System Inc.: SR 540). A thermoelectrically cooled laser diode (Suwtech LDC-1500) of 980 nm center wavelength, which was followed by a focus lens to control the pump beam size for mode matching, was used for excitation. The amplified seed beam was detected by an InGaAs detector (Newport 818-BB-30). The detected electric pulses were displayed by a digital oscilloscope (Agilent, infiniium 54833A DSO).

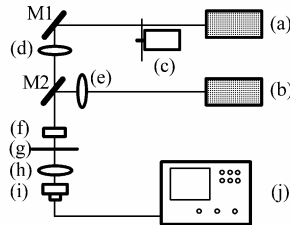


Fig. 2. The schematic diagram. (a) 1300 nm tunable laser diode as seed beam, (b) 980 nm laser diode as excitation resource, (c) chopper, (d) lens with 100 mm focal length, (e) lens with 50 mm focal length, (f) sample, (g) filter, (h) lens with 25 mm focal length, (i) InGaAs PIN detector and (j) digital oscilloscope. M1 and M2 are mirrors.

Figure 3 shows optical gain properties at 1300 nm. The optical gain increases linearly with excitation power up to 1.12 W. The inset shows an oscilloscope image of the amplification phenomenon with the excitation power of 1.12 W and the optical gain is calculated at 1.12. Optical gain coefficient is defined as:

$$g = 1/l \ln(I/I_0)$$

Where l is the thickness of glass sample and I/I_0 is optical gain. The optical gain coefficient is calculated to be about 0.283 cm^{-1} . The gain operation at 1300 nm has much significance since

it is at the second telecommunication window and it has minimum dispersion for silica optical fiber. So it has potential application in optical communication system.

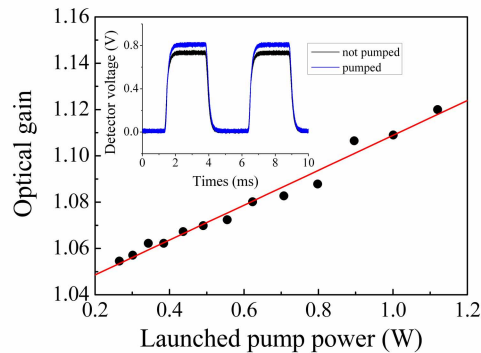


Fig. 3. Optical gain properties at 1300 nm. The inset shows an oscilloscope image of the amplification phenomenon.

Ni^{2+} -doped GC shows broadband near-infrared luminescence (see the inset of Fig. 4). In order to investigate its broadband amplification properties, the spectral dependence of optical gain was investigated. Figure 4 shows the results of optical gain as a function of different seed beam wavelength from 1272 to 1348 nm under excitation with 980 nm (the power is 1.12 W). Points and curve represents experimental measurements and fluorescence spectrum at 980 nm excitation. It can be seen that the measured spectral dependence of the optical gain appears to closely resemble the fluorescence spectrum. The optical amplification with 77 nm bandwidth indicates the present Ni^{2+} -doped GC may be potential for developing broadband optical amplifier and tunable laser. Additionally, the spectral dependence of optical gain is an important consideration if a fiber amplifier is to be incorporated in a broadband WDM system.

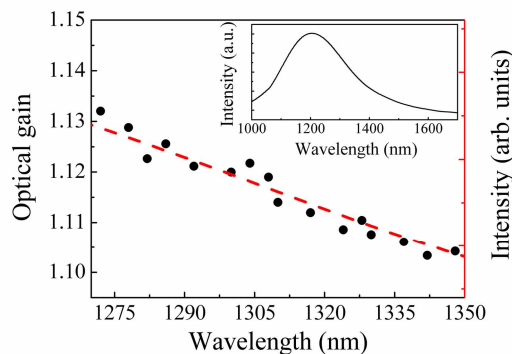


Fig. 4. Optical gain as a function of different seed beam wavelength from 1272 to 1348 nm (the excitation power is 1.12 W). Points and curve represents experimental measurements and fluorescence spectrum at 980 nm excitation (the inset gives the whole fluorescence spectrum).

The realization of optical amplification in Ni^{2+} -doped $\beta\text{-Ga}_2\text{O}_3$ GC might be attributed to the improvement of the optical properties. Numerous researches have showed that TM ions luminescence is strongly baffled by nonradiative process and the local arrangement around TM ions, i.e. crystal field environments, take an important role [9-11]. The variation of crystal field environment can be explained by utilizing the crystal field parameters Dq and the Racah parameters B and C , which were determined by solving the Tanabe-Sugano matrix according to absorption spectrum [12]. The comparison of crystal field parameters and luminescent decay time for Ni^{2+} in $\beta\text{-Ga}_2\text{O}_3$ GC and ever reported GC materials are summarized in table 1. The variation of Dq/B values and fluorescent lifetime follows the order:

β -Ga₂O₃ GC > LGS GC [4] > ZAS GC [3] > MGTS GC [13]

To explain the experimental results, we employed the simplified Mott model about the probability of nonradiative transition [14], which obeys the activation energy relation:

$$W_{\text{nrad}} \sim W_0 \exp(-\Delta / kT)$$

Where W_0 is a constant, Δ is the energy gap and for ${}^3T_2(F)$ - ${}^3A_2(F)$ transition it is the energy difference between the bottom of the ${}^3T_2(F)$ level and the intersection of the parabolas of the ${}^3T_2(F)$ and ${}^3A_2(F)$ levels, k is the Boltzmann constant, and T is the temperature. According to the Tanabe-Sugano energy levels diagram the ${}^3A_2(F)$ level is independent on the Dq/B value but the ${}^3T_2(F)$ level changes with the Dq/B parameter. As a result, the larger Dq/B value, the larger the activation energy Δ will be. This means that if Ni²⁺ occupies the strong crystal field sites, the nonradiative rates will be smaller, which results in intense luminescence and long fluorescent lifetime. The same conclusion can be acquired if a tunneling process between the ${}^3T_2(F)$ and ${}^3A_2(F)$ levels accounts for the nonradiative transitions. On the other hand, the phonon energy of matrix might affects the probability of nonradiative decay of active ion dopants [15]. The moderate phonon energy of β -Ga₂O₃ (767 cm⁻¹) also favors radiative transition process of Ni²⁺.

Table 1. Comparison of optical properties and crystal field parameters for Ni²⁺ in β -Ga₂O₃ GC and ever reported GC materials.

	β -Ga ₂ O ₃ GC	LGS GC*	ZAS GC [§]	MATS GC [†]
Dq(cm ⁻¹)	989	948	907	885
B(cm ⁻¹)	892	895	940	961
C(cm ⁻¹)	3237	3141	3919	-
τ (μ s)	665	583	200	122

* LiGa₅O₈ GC, ref.[4]; § ZnAl₂O₄ GC, ref.[3]; † MgAl₂Si₃O₁₀ GC, ref.[13]

The gain system has many attractive features. In comparison with crystal, TM-doped GC can be easily fabricated into optical fibers keeping the optical active of TM ions [16]. In present system, the silicate-based GC with broadband amplification at 1300 nm telecommunication window when it is excited with a common commercial semiconductor laser (980 nm), which implies this materials can overcome the disadvantages of the present Praseodymium-doped fluoride fiber amplifiers (PDFFAs) such as brittle and narrow amplification bandwidth (25 nm) [17, 18]. The broadband amplification and long fluorescent lifetime have potential applications in ultrashort-pulses generation and high-power laser. The optical gain can be improved by increase the pump power. At present, we have got twofold gain in bulk GC when the pump power is 7 W.

4. Conclusion

In summary, we demonstrated broadband optical amplification near the 1300 nm region for silicate GC containing β -Ga₂O₃:Ni²⁺ nanocrystals. The amplification bandwidth was 77 nm and it can be expected to be broader. The optical gain shows similar wavelength dependence to luminescence properties. The available spectroscopic data such as long fluorescent lifetime and broadband amplification shows the present GC system has potential applications in broadband optical fiber amplifiers and tunable lasers.

Acknowledgments

The authors would like to acknowledge the financial support provided by the National Natural Science Foundation of China (Grant No. 50672087) and National Basic Research Program of China (2006CB806000b).